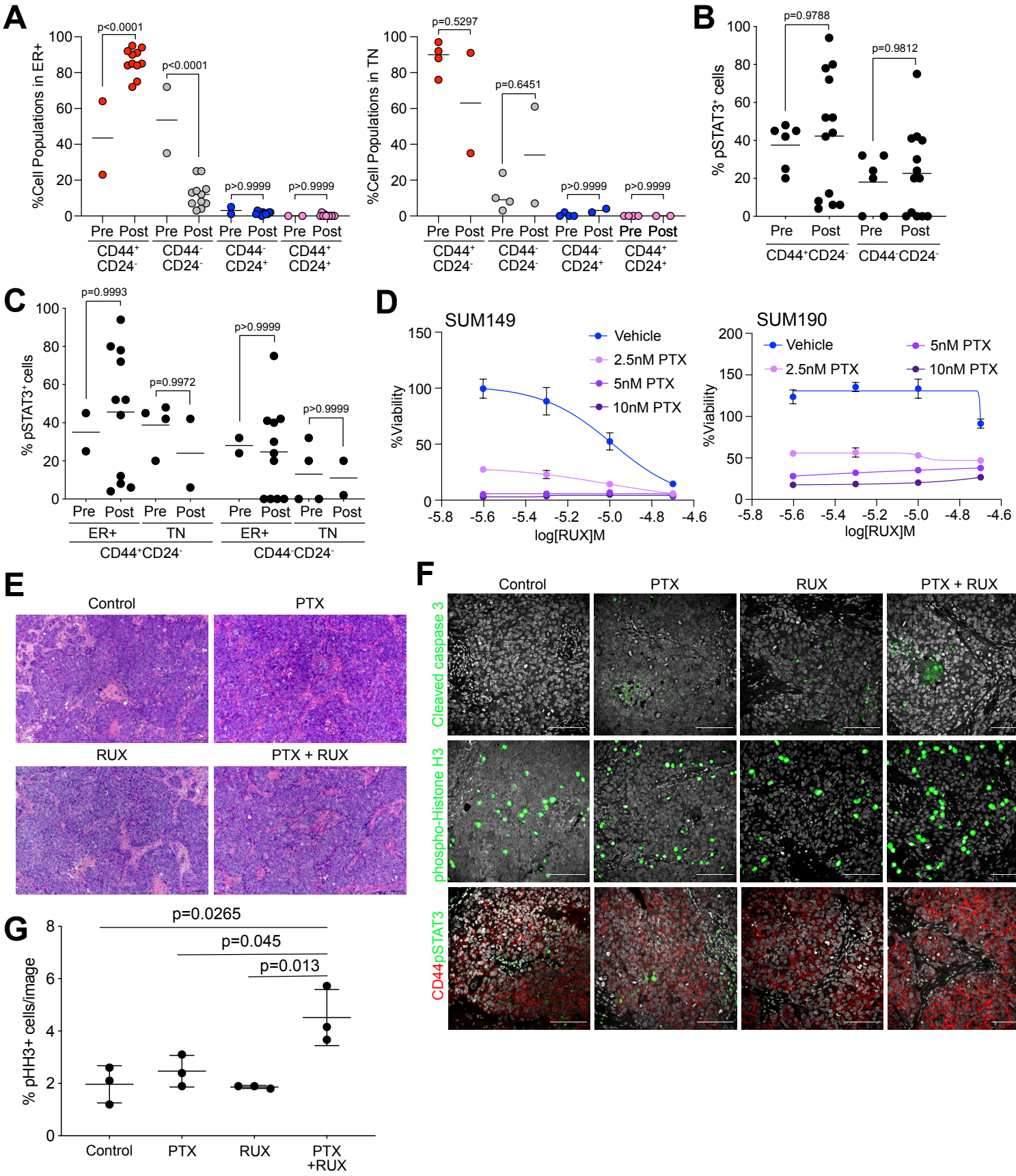

Supplementary Fig S1

Supplementary Fig. S1. Analysis of IBC tumors and xenografts. A, Frequency of each of the four cell types ($CD44^+CD24^-$, $CD44^-CD24^-$, $CD44^-CD24^+$, and $CD44^+CD24^+$) in ER+ (left) and triple-negative (TN, right) cases that were pre or post treatment. **B,** Percent $pSTAT3^+$ cells in $CD44^+CD24^-$ or $CD44^-CD24^-$ cell subpopulations in pre vs. post treatment. **C,** Percent $pSTAT3^+$ cells in $CD44^+CD24^-$ or $CD44^-CD24^-$ cells pre vs post treatment in ER+ or TN subtypes. All p-values for A-C were calculated by Tukey's multiple comparisons test after one-way ANOVA. **D,** Cell viability after treatment with different doses of ruxolitinib (RUX) and paclitaxel (PTX) normalized to vehicle controls in SUM149 and SUM190 cell lines. Error bars represent s.d. (n=3). **E,** Representative images of hematoxylin-eosin-stained slides of SUM190 xenografts. Scale bar = 100μm. **F,** Representative images of immunofluorescence analyses for the indicated markers in SUM190 xenografts. DAPI shown in gray. Scale bar = 50μm. **G,** Graph depicting quantification of phospho-histone H3 immunofluorescence signal. p-values calculated by students t-test (n=3).

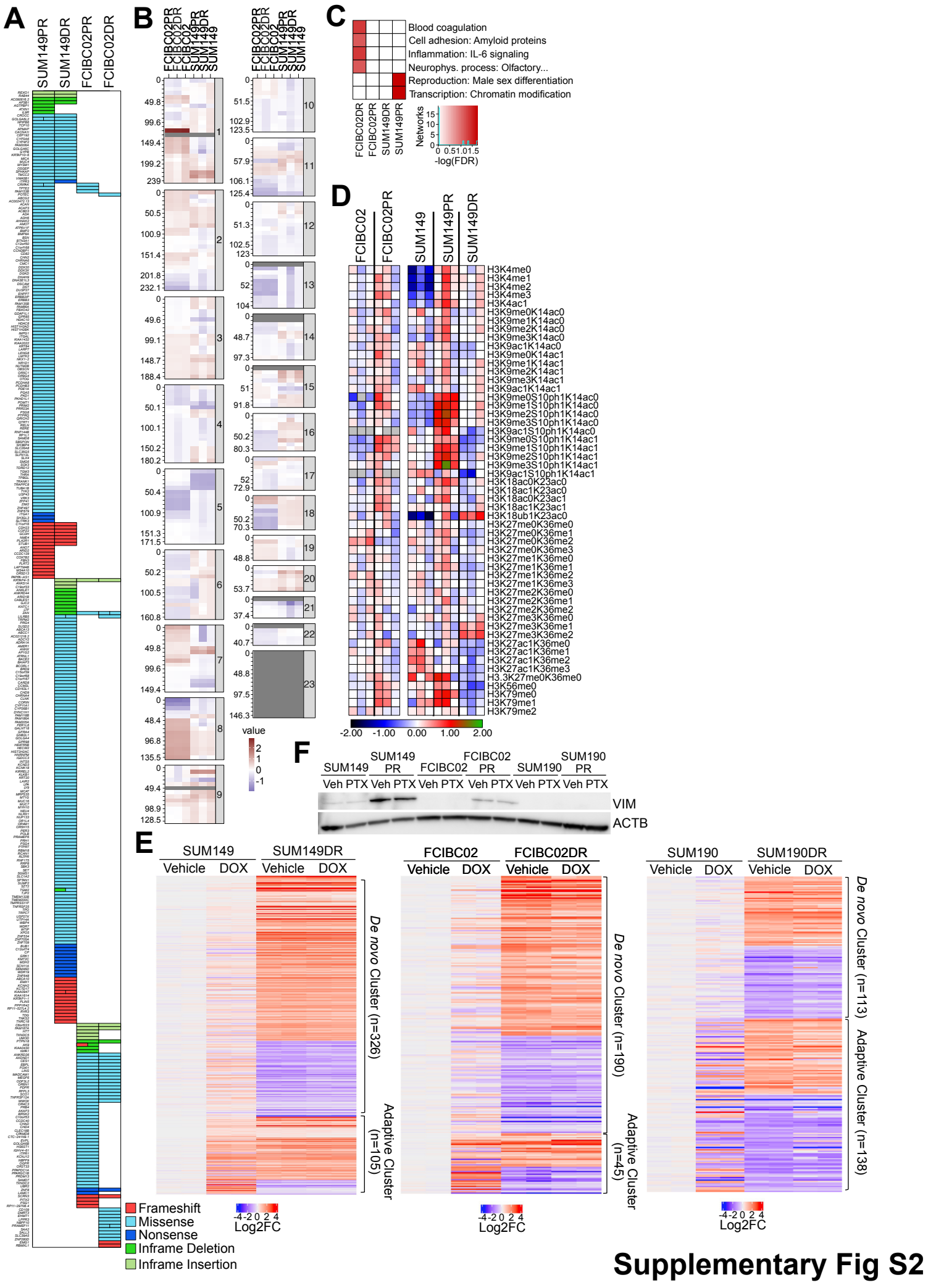

Supplementary Fig S2

Supplementary Fig. S2. Characterization of drug-resistant IBC cell lines. A, Mutations detected in the indicated resistant cell lines with an allelic fraction > 0.1 and not in their corresponding parental cell line. Colors indicate frameshift, missense, nonsense, inframe insertions, and deletions. **B,** CNV analysis of indicated cell lines shown in 10MB intervals across chromosomes. **C,** Process networks significantly enriched (FDR < 0.1) in at least one cell line in genes with genetic alterations specific to the indicated resistant cell line. Color scale corresponds to -log(FDR) of significance of enrichment, calculated by MetaCore Enrichment Analysis test. **D,** Heatmap of histone mass spectrometry data in the indicated cell lines. Data is row median normalized for each histone mark within each cell line set. **E,** Heatmap of significant differentially expressed genes in the indicated cell lines between parental and resistant derivatives clustered by either their presence (adaptive cluster) or absence (*de novo* cluster) in parental doxorubicin-treated (DOX) cells compared to vehicle. **F,** Immunoblot analysis for vimentin (VIM) following 24hrs of Vehicle or Paclitaxel (PTX) treatment in each cell lines respective IC50 for PTX. ACTB was used as loading control.

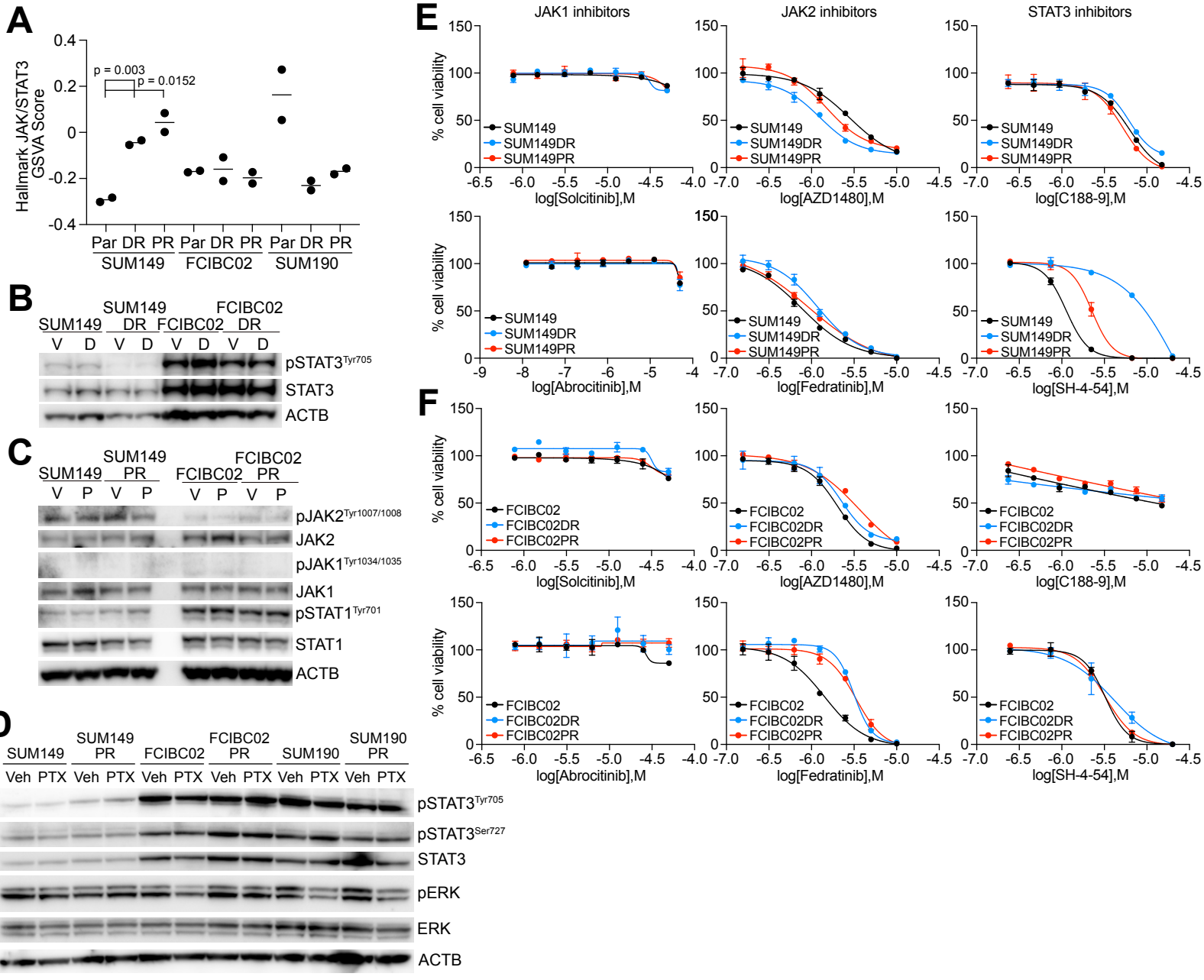

Supplementary Fig S3

Supplementary Fig. S3. Interrogation of the JAK/STAT pathway in resistant derivatives. A, Gene Set Variation Analysis (GSVA) score showing relative enrichment of the Hallmark IL6/JAK/STAT3 gene signature in the indicated cell line from RNA-seq data generated in **Fig. 2**. p-values calculated by students t-test. **B,** Immunoblot analysis for pSTAT3 and STAT3 in the indicated cell lines following 24hrs of vehicle (V) or doxorubicin (D) treatment. ACTB was used as loading control. **C-D,** Immunoblot analysis for components of the JAK/STAT pathway in indicated cell lines following 24hrs treatment of Vehicle (V) or Paclitaxel (P) treatment. ACTB was used as loading control. **E-F,** Cellular viability following treatment with indicated inhibitors targeting different components of the JAK/STAT pathway. Error bars represent s.d., n=3. Representative dose-curves are shown of experiments repeated 2-3 times.

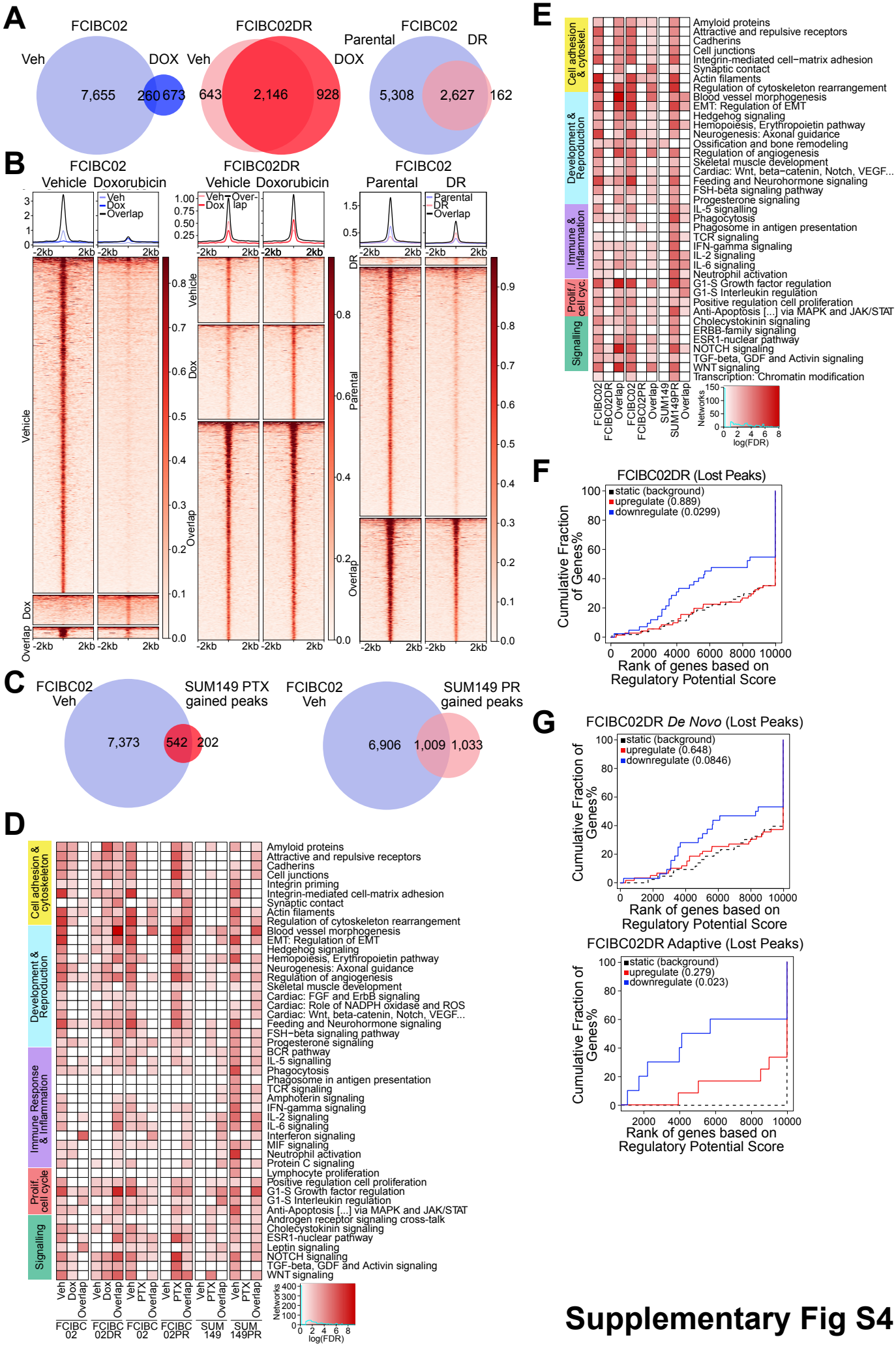

Supplementary Fig S4

Supplementary Fig. S4. Characterization of STAT3 chromatin binding. A, Venn diagram depicting overlap of pSTAT3^{Tyr705} peaks between vehicle (Veh) and doxorubicin (Dox) treated FCIBC02 and FCIBC02DR cells. **B,** Heatmap depicting pSTAT3^{Tyr705} peaks which are unique in vehicle (Veh) and doxorubicin (Dox) treated FCIBC02 and FCIBC02DR cell lines and the overlap between groups. The color key is the score of the ChIP-seq signal over the selected genomic region, and the signals across different genomic regions have been scaled to the same length. **C,** Venn diagram depicting overlap of pSTAT3^{Tyr705} peaks in FCIBC02 parental cells with peaks gained in paclitaxel treated SUM149 cells compared to vehicle (left) or SUM149PR cells compared to parental (right). **D-E,** Process networks in each ChIP-seq comparison following 24hrs of indicated treatment (**D**) or vehicle treated parental and resistant derivatives (**E**) that were significantly enriched (FDR < 0.001) in pSTAT3 targets. Color scale corresponds to -log(FDR) as calculated by Metacore. **F,** Integration of differential gene expression and pSTAT3^{Tyr705} targets by BETA analysis. The p-value listed in the top left represents the significance of the up or down group relative to the unchanged (NON) group as determined by the Kolmogorov-Smirnov test. **G,** BETA analysis of differentially expressed genes in the adaptive or *de novo* clusters from **Supplementary Fig. S2E** and pSTAT3^{Tyr705} targets in FCIBC02DR cells.

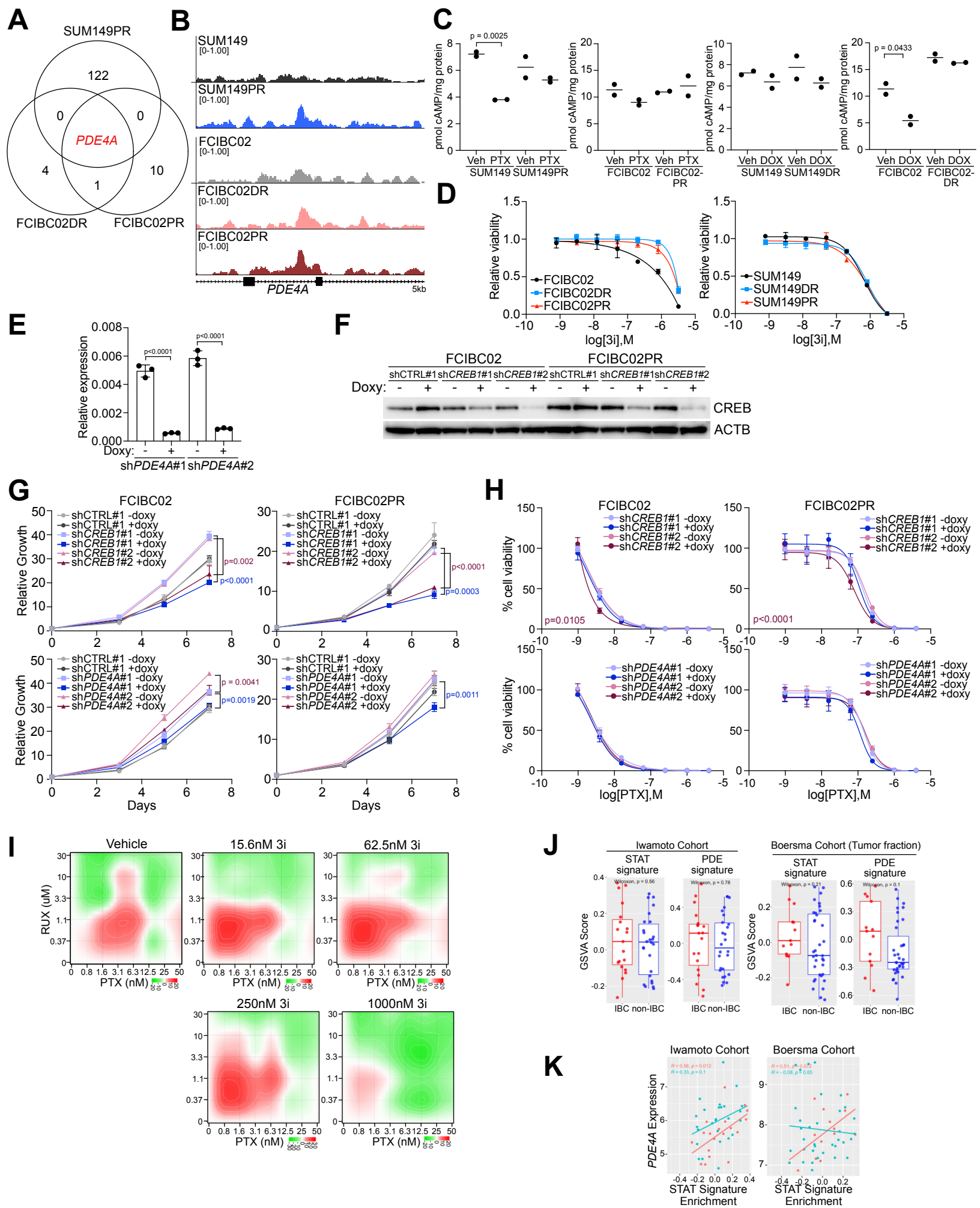

Supplementary Fig S5

Supplementary Fig. S5. Metabolic changes in IBC resistant derivatives and in IBC patient samples. A, Overlap of genes that are both upregulated (RNA-seq) in resistant vs. parental cells and are pSTAT3 targets (ChIP-seq) only in resistant cell lines in SUM149PR, FCIBC02DR, and FCIBC02PR. *PDE4A* is the only gene that is both a pSTAT3 target only in resistant lines and has higher mRNA levels in resistant derivatives. **B,** Gene tracks of pSTAT3 signal at the *PDE4A* genomic locus that was found to be differentially bound in resistant vs. parental comparisons. x-axis depicts position along the chromosome with gene structure drawn below. y-axis shows genomic occupancy in units of rpm/bp. **C,** ELISA for cAMP normalized to total mg protein in the indicated cell lines treated with vehicle (Veh), paclitaxel (PTX), or doxorubicin (DOX) for 72hrs (n = 2). **D,** Cellular viability of indicated cell lines treated with the CREB inhibitor 3i. Error bars represent s.d., n = 3. **E,** mRNA expression of *PDE4A* normalized to *GAPDH* as measured by quantitative RT-PCR in FCIBC02 dox-inducible sh*PDE4A* cell lines treated for 72hrs with and without 1ug/ml doxycycline (doxy). **F,** Immunoblot analysis for CREB in FCIBC02 and FCIBC02PR cells expressing dox-inducible sh*CREB1* treated with and without 1ug/ml doxycycline (doxy) for 72hrs. ACTB was used as loading control. **G,** Cell viability analysis in indicated cell lines grown with and without doxycycline (doxy). Error bars represent s.d., n=3, p-values determined by student's t-test. **H,** Cellular viability after 7 days of paclitaxel treatment in the presence or absence of doxycycline (doxy) in the indicated cell lines. Error bars represent s.d., n=3. p-values determined by comparison of fits using F test. **I,** Plots of synergy scores for SUM149PR cells treated with paclitaxel (PTX) and ruxolitinib (RUX) in combination with increasing doses of the CREB inhibitor 3i (n=3). Synergy was calculated using the ZIP model where a score of 0 denotes an additive response, while areas of red and green indicate synergism and antagonism, respectively. **J,** STAT and PDE-family gene signature scores in Boersma or Iwamoto patient cohorts with both IBC and non-IBC samples. **K,** Correlation plots from datasets in panel J between STAT signature from KEGG and PDE4A gene expression.

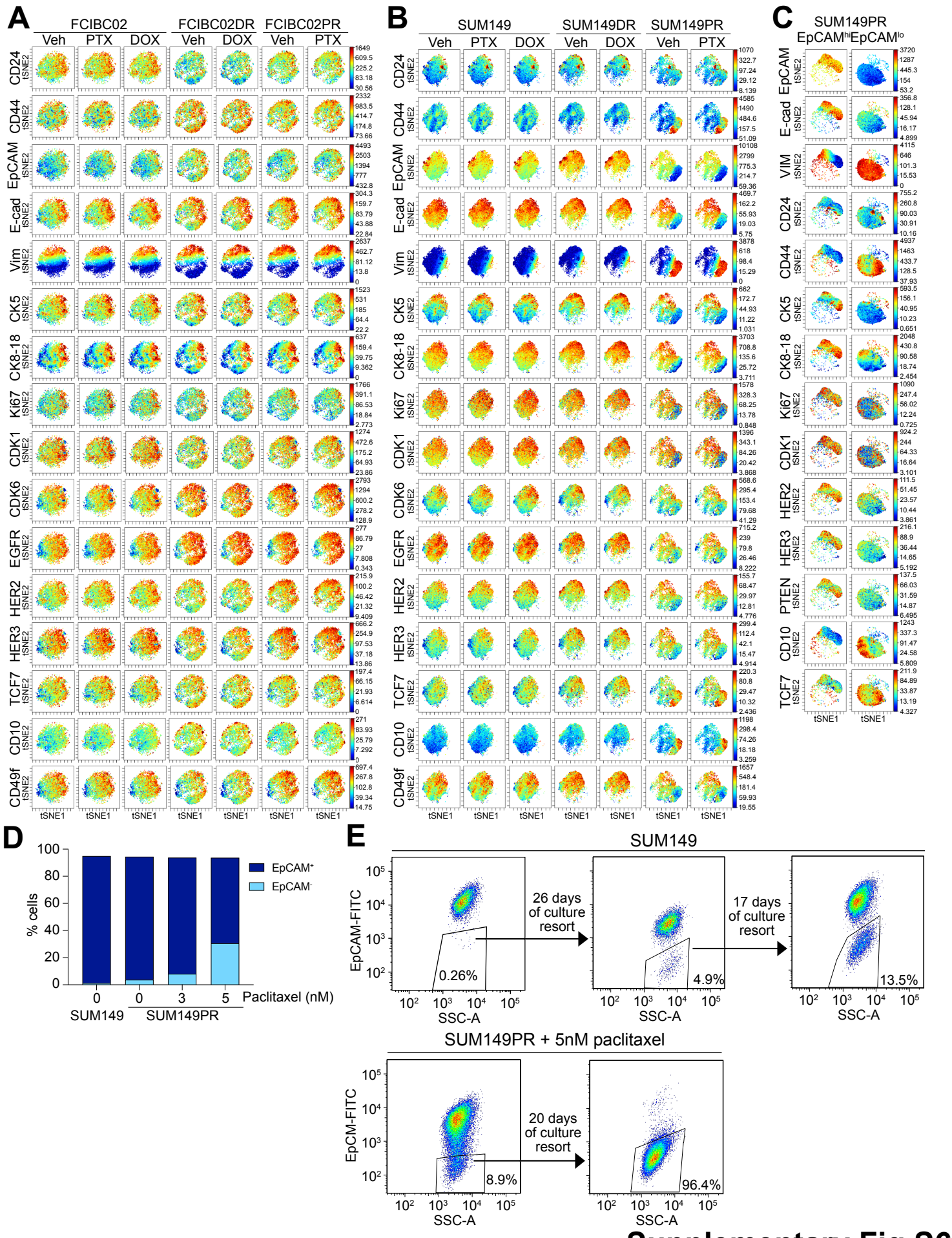

Supplementary Fig S6

Supplementary Fig. S6. Cellular heterogeneity of IBC cell lines. A-B, viSNE maps from CyTOF analysis of parental FCIBC02 cells (**A**) or SUM149 cells (**B**) and their resistant derivates after vehicle (Veh), paclitaxel (PTX), or doxorubicin (DOX) treatment. Color scale indicates minimum and maximum values of expression. **C,** CyTOF analysis of SUM149PR cells gated for $EpCAM^{hi}$ and $EpCAM^{low}$ populations and then shown in viSNE maps for differentially expressed markers. **D,** Graph depicting relative fraction of $EpCAM^{+}$ and $EpCAM^{-}$ cells based on FACS following paclitaxel treatment in SUM149 and SUM149PR cells. **E,** FACS sort of initial population of SUM149 and SUM149PR cell lines for EpCAM expression (left panel). Cells within gate were then grown in cell culture for the indicated number of days and resorted for EpCAM expression (middle panel). For SUM149, cells were grown for the indicated number of days and analyzed by FACS for EpCAM expression (right panel). Percentages indicate the cells gated as $EpCAM^{-}$.

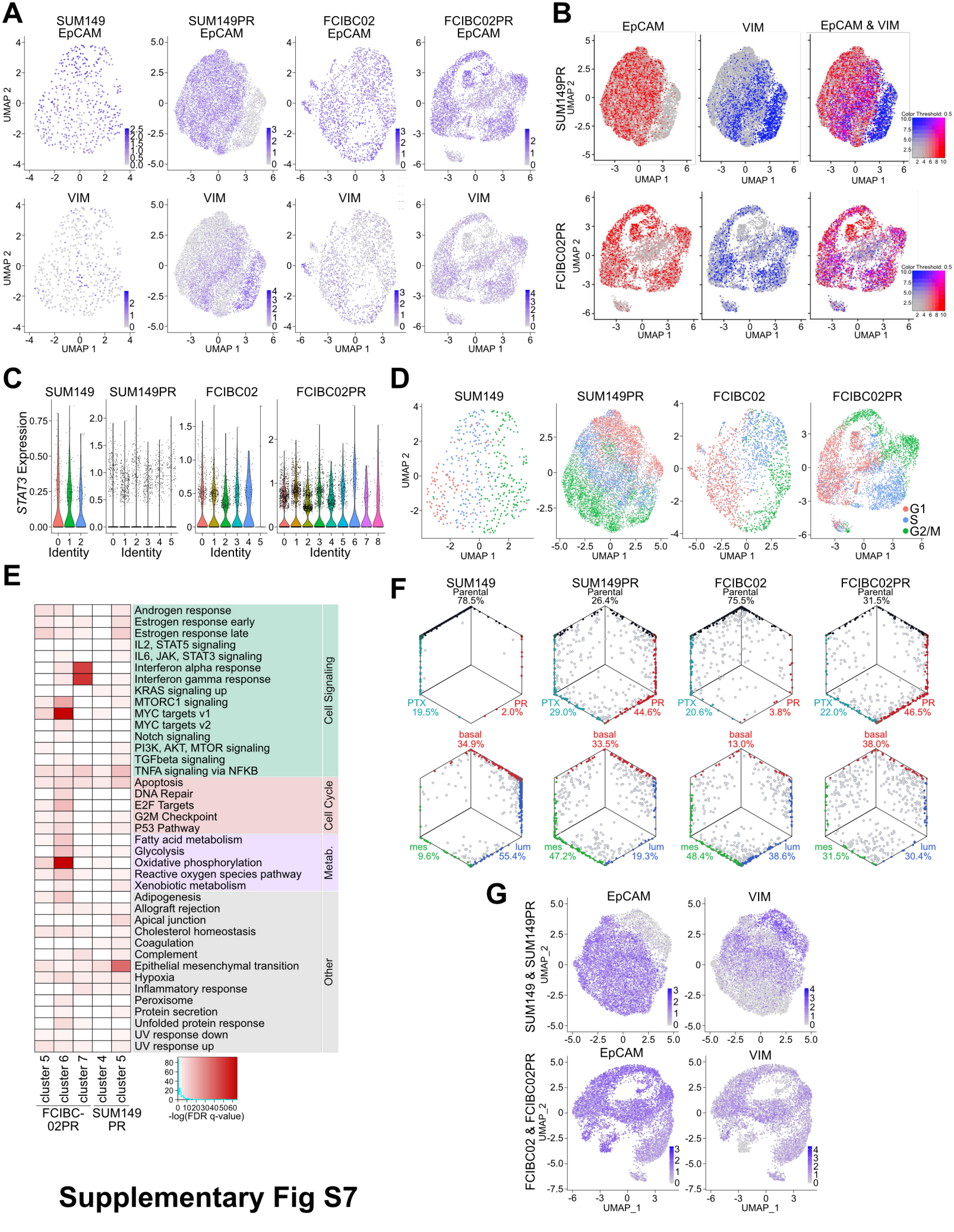

Supplementary Fig S7

Supplementary Fig. S7. Heterogeneity of paclitaxel resistant derivatives. A, UMAP plots of single cell RNA-seq (scRNA-seq) data in the indicated cell lines. Cells are colored based on the expression of EpCAM (top) or Vimentin (bottom). **B,** UMAP plots of scRNA-seq data in SUM149PR (top) and FCIBC02PR (bottom). Cells are colored based on the expression of EpCAM (red) and VIM (blue). Right plot depicts overlap of EpCAM and VIM expression according to color threshold shown on the right, where purple cells indicate the hybrid-EMT cell state. **C,** Violin plots of scRNA-seq data by cluster (corresponding to clusters in Figure 5E) of STAT3 expression levels. **D,** UMAP plots of scRNA-seq data in indicated cell lines. Cells are colored based on cell cycle phase. **E,** Gene set enrichment analysis of genes defining the indicated clusters (as determined in **Fig. 5E**) that were significantly enriched (FDR < 0.05) for hallmark gene sets in at least one cluster. Color scale indicates -log(FDR q-value). **F,** Hexagonal plots analyzed by an alternative method to **Fig 5I-J** with classifications based on gene z-scored expression data. Top panel, single cells were classified as either parental (black), paclitaxel-treated parental (PTX, teal), or paclitaxel resistant (red). Bottom panel, single cells were classified as either basal (red), mesenchymal (green), or luminal (blue). Gray cells are unclassified and mixed colors represent cells that belong to both classifications. Percentages indicate cells assigned to each classification. **G,** UMAP plots of integrated scRNA-seq data for SUM149/SUM149PR (top) and FCIBC02/FCIBC02PR (bottom) cells colored based on expression of EpCAM or vimentin.

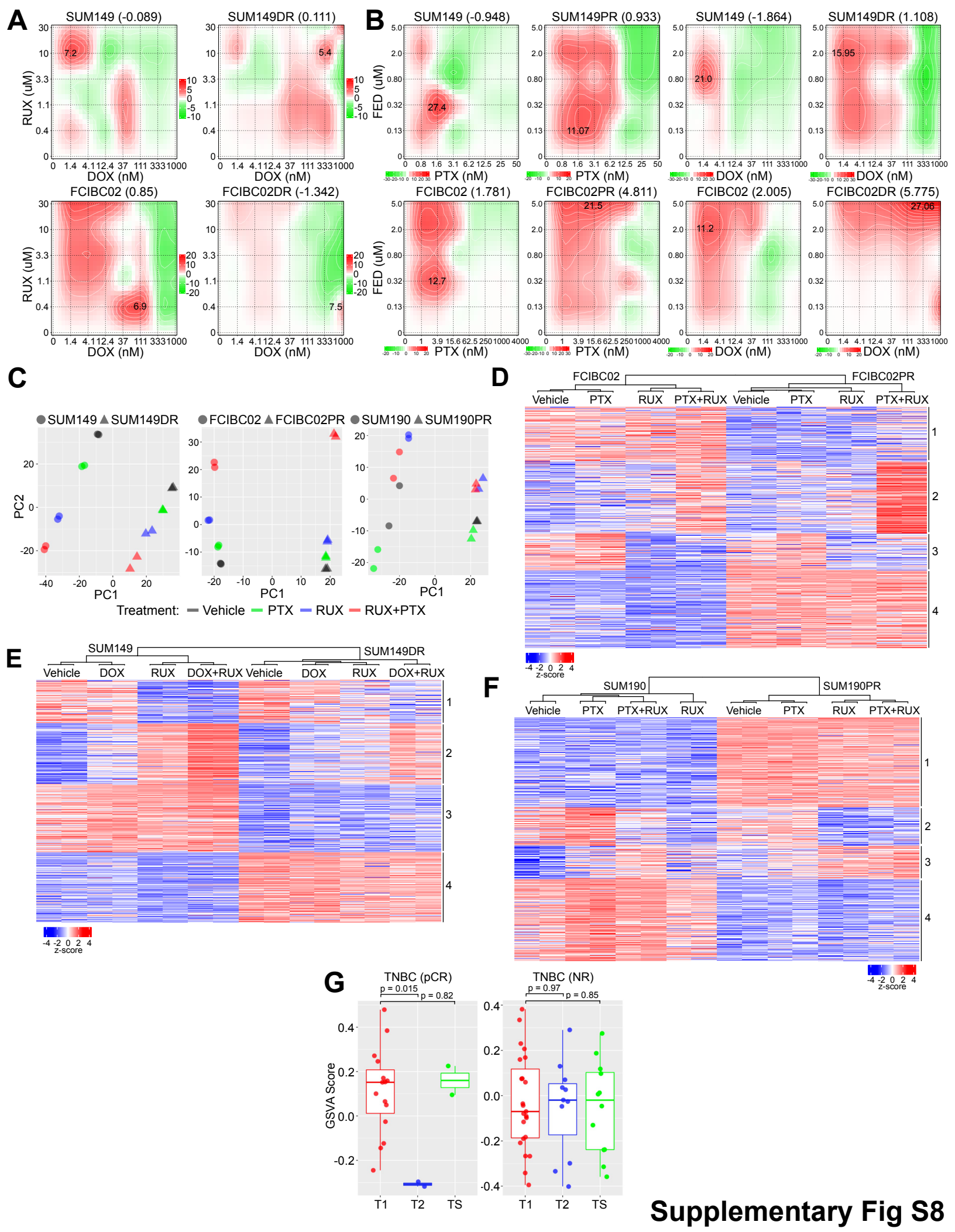

Supplementary Fig S8

Supplementary Fig. S8. Synergy between JAK2 inhibitor and chemotherapeutic agents. A, Synergy plots for doxorubicin (DOX) and ruxolitinib (RUX) treatment in the indicated cell lines calculated by ZIP model, where a score of 0 indicates an additive response and areas of red and green indicate synergistic and antagonistic doses, respectively. **B,** Synergy plots for fedratinib (FED) in combination with either doxorubicin (DOX) or paclitaxel (PTX) and analyzed as in panel A. **C,** PCA plot of RNA-seq data of SUM149 parental and SUM149DR cells (left) or FCIBC02 parental and FCIBC02PR cells (middle) and SUM190 parental and PR cells (right) treated with single agents or the combination. **D,** Heatmap of gene expression changes in FCIBC02 and FCIBC02PR cells after Veh, PTX, RUX, or PTX+RUX treatment for 72hrs. **E,** Heatmap depicting gene expression changes in SUM149 and SUM149DR cells after DOX, RUX, and combined treatment for 72hrs. **F,** Heatmap of gene expression changes in SUM190 and SUM190PR cells after PTX, RUX, and combined treatment for 72hrs. **G,** IBC-STAT gene signature in TNBC patient samples from the I-SPY trial and stratified by time point of sampling (T1 = prior to treatment, T2 = 24-96 post chemotherapy and TS = surgery) and patient outcome (pCR = complete pathologic response, NR = nonresponder). Differences calculated by Wilcoxon-rank sum test.

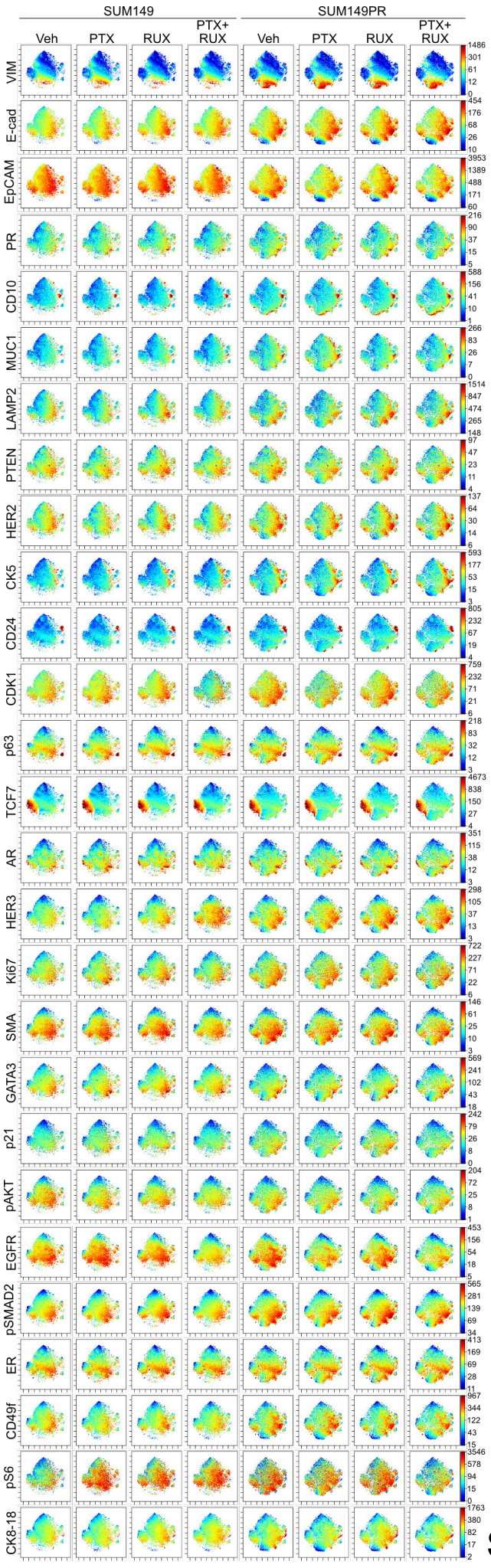

Supplementary Fig S9

Supplementary Fig. S9. Combination treatment decreases emergence of EMT-resistance phenotype. viSNE plots of CyTOF analysis of SUM149 and SUM149PR cells treated with vehicle (Veh), paclitaxel (PTX), ruxolitinib (RUX), or the combination (PTX + RUX) for 14 days. Plots are colored for the expression of the indicated marker.

SUPPLEMENTARY TABLES

Supplementary Table S1. List of genes used in gene signatures.

Supplementary Table S2. List of tumor samples.

Supplementary Table S3. Results of exome-seq.

Supplementary Table S4. Results of Pathway analyses.

Supplementary Table S5. List of genes differentially expressed after single agent treatments.

Supplementary Table S6. List of pSTAT3 genomic targets based on ChIP-seq.

Supplementary Table S7. Metabolites measured by LC-MS/MS.

Supplementary Table S8. List of genes differentially expressed among clusters in scRNA-seq data.

Supplementary Table S9. List of genes differentially expressed after combination treatments.